Evaluation of a microclimate simulation tool on an experimental mock-up and passive cooling strategies assessment

Alexandre Bryk, Emmanuel Bozonnet, Peter Riederer, G-E Kyriakodis

P. Rajagopalan, V. Soebarto and H. Akbari (Eds.), *6th International Conference on Countermeasures to Urban Heat Islands (IC2UHI)*, pp. 1027-1036. ©2023, RMIT University, Melbourne, Australia

Evaluation of a microclimate simulation tool on an experimental mock-up and passive cooling strategies assessment

Alexandre Bryk[1,2], *Emmanuel Bozonnet*[2], *Peter Riederer*[3], *Georgios Kyriakodis*[4]
[1,3,4]*Centre Scientifique et Technique du Bâtiment, Sophia Antipolis, France*
[1,2]*LaSIE, La Rochelle Université, France*

ABSTRACT

This paper presents an experimental verification of a coupled simulation model originating from EnviBatE (microclimate tool) and the urban building energy model (UBEM) Dimosim. Based on synchronous coupling techniques, the microclimate model considers detailed solar radiations and airflow calculations as well as a zonal model for discretized canopy air nodes and building nodes. A reduced-scale experimental mock-up provides the possibility to carry out the evaluation of the tool against on-site measurements. The mock-up consists of five rows of empty concrete blocks on a 1:10 scale with an aspect ratio of 1.2. For calibration and validation purposes, we collected measurements of surface and air temperatures, incident solar radiation and incident longwave radiation coming from the sky. Then, we compare outdoor and indoor temperature of the experimental mock-up and the numerical model for a monitoring period of 26 days. The analysis highlights the capabilities of the coupled model to represent the urban canyon effects. This study allows quantifying the effects of reflective coatings in order to reduce local overheating on a neighborhood scale.

Keywords: Microclimate simulation, UBEM, experimental mock-up, model validation

Introduction

Urban microclimate affects indoor and outdoor conditions, influencing both the energy demand of buildings (Allegrini et al. 2012) and the outdoor comfort of people and ensuring both goals can be contradictory, for example Erell et al. (2014) argue that high-albedo materials can degrade thermal comfort at the pedestrian level but underline their potential for energy savings. Numerical models can enable to simultaneously assess indoor and outdoor environments, determine heat exposure, and evaluate cooling strategies. However, the parameterization of such models requires a lot of information that may affect the reliability of the results. A verification or calibration against measurements is then required to verify the validity of the models. One study proposes an automated calibration process for the geometrically simplified Urban Weather Generator model (Mao et al. 2018) where the calibration is performed on the air temperature. Nevertheless, this methodology is hardly feasible for detailed microclimate models, which require much more time-consuming computations. Another study by Detommaso et al. (2021) focuses on calibrating the detailed Envi-met microclimate model by providing more refined input data that capture site-specific effects. Many uncertainties exist due to the large number of parameters, often uncontrolled such as anthropogenic heat flux.

[1] Corresponding Author: [alexandre.bryk@cstb.fr]
[2] [emmanuel.bozonnet@univ-lr.fr]
[3] [peter.riederer@cstb.fr]
[4] [Georgios.kyriakodis@cstb.fr]

Other studies have addressed this problem with reduced scale mock-ups of neighborhoods that correctly reproduce the radiative processes that occur, but do not reproduce all the similarities between the full-scale and reduced-scale mock-up (Doya et al. 2012) in terms of air flow around buildings. A first configuration presented by Pigliautile et al. (2020) consists of about twenty concrete blocks of variable length and height between 2.4 and 5m arranged to avoid shading between buildings in a continental Mediterranean climate. The configuration is equipped with green walls and a numerical simulation evaluates white coatings. Another study by Salvati et al. (2022) reproduced an existing district at a scale 1:10 and showed that the compatibility between indoor and outdoor thermal comfort objectives should be carefully considered when applying reflective coatings. In a canyon model at 1:2 scale, Athamena et al. (2018) validate a microclimate model by also focusing on the multiple wind field.

All these studies have several limitations. First, the limited number of calibration points and often limited to air temperature. A study by Krayenhoff et al. (2021) points out that air temperature may not be sufficient. To study thermal comfort, other parameters such as mean radiant temperature need to be validated by surface temperatures or by calibrating the numerical radiation algorithms. This study proposes a methodology for calibrating a numerical microclimate model on a reduced-scale mock-up with the available in-situ sensors and outlines the limitations of some boundary conditions on the evaluation of variables that drive thermal comfort.

Experimental mock-up

The experimental mock-up used for the validation is located at the University of La Rochelle, France (46°10N, 01°07W). It consists of five rows of three empty tanks placed on a 10x20m terrace of concrete slab terrace. Each row is 5 m long, 1.3m high and 1.12 m wide with a canyon width of 1.2 m. A fifth canyon corresponds to a wall of the same height as the blocks. The aspect ratio for each canyon is approximately equal to 1.2. This mock-up has already been studied to assess the impact of cool paintings on the microclimate. The impact of green envelopes is being evaluated in (Djedjig, Bozonnet, & Belarbi 2015). The mock-up is located near the sea but is protected by a row of trees that attenuate the wind coming from the sea on the west and nearby buildings on the east as described by Doya et al. (2012).

The mock-up is equipped with sensors to measure air temperatures, surface temperatures, incoming solar radiation, reflected solar radiation, incoming longwave radiation from the sky and emitted longwave radiation from specific canyons. A weather station installed on the roof of the nearby university collects meteorological data. The sensors installed on the mock-up used in this study are type K thermocouples (chromel-alumel) with an uncertainty of 0.3°C for air and surface temperatures. A pyranometer (Kipp & Zonen CMP3, spectral waveband 310-2800 nm, field of view 180°) and a pyrgeometer (Kipp & Zonen CGR3, spectral waveband 4500 -42 00nm, field of view 150°) are placed above the canyon to measure the reflected solar radiation and the longwave emittance of the roads respectively. A hygrometer (Campbell Scientific CS215 temperature and RH sensor) placed in the center of the canyon simultaneously measures air temperature (± 0.4°C between 5 and 40°C) and relative humidity (± 2% between 10 and 90% RH). A 2D sonic anemometer (WindSonic^{TM}) is placed on the building of interest at a height of 28cm and measures wind speed (0-60 m/s ± 2% at 12m/s) and wind direction (±3° at 12m/s).

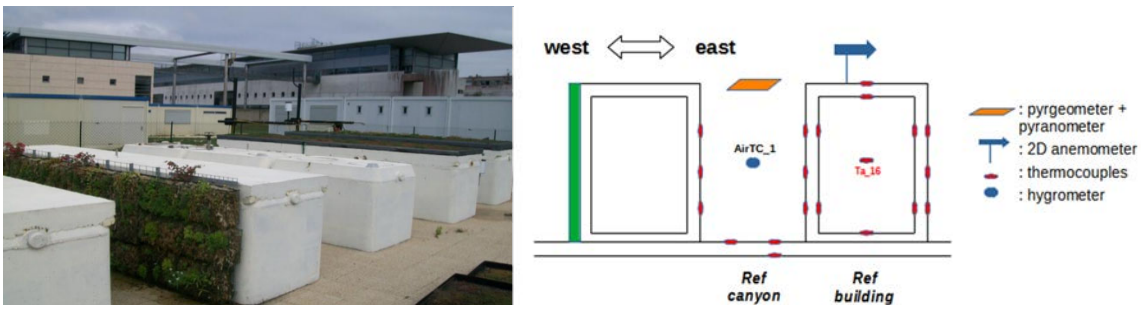

Figure 1. Experimental mockup Climabat (left) and the area of interest (right)

To calibrate the numerical model, a specific canyon and a set of buildings have been chosen for calibration Figure 1. These are the farthest from the vegetation and are not affected by its presence, as we do not consider vegetation in this study. The parameters determined in previous studies include the thermal properties of the concrete representing buildings, as well as the properties of the concrete tiles.

Simulation tools: DIMOSIM and EnviBatE

Dimosim or District MOdeller and SIMulator (Garreau et al. 2021) is an Urban Building Energy Model following an bottom-up approach. It calculates the energy demand and consumption of buildings and their energy system by taking into account the energy systems such as heat pumps or thermal networks at the district scale. The part of interest here is the building model which considers the following physical phenomena: indoor and outdoor convective heat exchange between air and surfaces, heat conduction of heat through external walls, inertia of internal walls and floors, absorption of solar radiation by opaque and semitransparent surfaces, transmission of solar radiation through windows and redistribution, and long-wave exchanges with the sky and the ground. Since the heat exchange between zones is not considered in the version used here, the thermal calculation of each thermal zone is independent.

EnviBatE or Environment and Buildings is a microclimate model that couples the solar radiation algorithm SOLENE (Groleau, Fragnaud, & Rosant, 2003) with the urban wind CFD model QUIC (Singh, Hansen, Brown, & Pardyjak 2008). The former calculates the direct and diffuse components of solar radiation using the radiosity method to determine the multiple reflections between facets. It also calculates view factors between planar surfaces. The second tool, QUIC, uses empirical parameterization of the mock-up for wind estimation. The results of both tools are integrated into a unique zonal mesh that estimates outdoor comfort metrics.

DIMOSIM replaces the building model of the EnviBatE model using a socket coupling technique which has been developed by Kyriakodis (2020). The coupling strategy used here is a zone-to-zone information exchange: at each time step, the calculated air temperature from EnviBatE, and the infrared radiation with other surface temperatures weighted by their respective view factors are considered as boundary conditions for the current time step in the corresponding thermal zone of DIMOSIM. The latter calculates surface temperatures of the building envelopes and system heat fluxes for the corresponding boundary conditions in the next time step of EnviBatE. The two packages exchange information sequentially at each time step using a ping-pong scheme. However, DIMOSIM has the ability to iterate at each time step before sending data through sockets which is necessary for iterative models or procedures.

Calibration of the model

The digital mock-up is based on the geometry of the real mock-up scaled by a factor of 7.2. On the one hand, this is due to a limitation of the software, which imposes a height of 3m

for a zonal mesh for both outdoor air zones and building zones. On the other hand because the building is modeled by three floors to match the number of thermocouples on vertical facades. This choice creates three virtual zones inside the building volume with three different thermal balances. In order to homogenize the indoor air temperature, a constant mixed air flow of 6 vol/h is imposed between the three zones of numerical model. This value is chosen to ensure a maximum air temperature difference of 1°C between the upper and lower zones. The digital mock-up consists of 321 number of facets and 654 outdoor zone meshes. Figure 2 shows the mock-up with its corresponding surface mesh. The zonal mesh follows the geometry of the ground with a constant z-axis height of three meters.

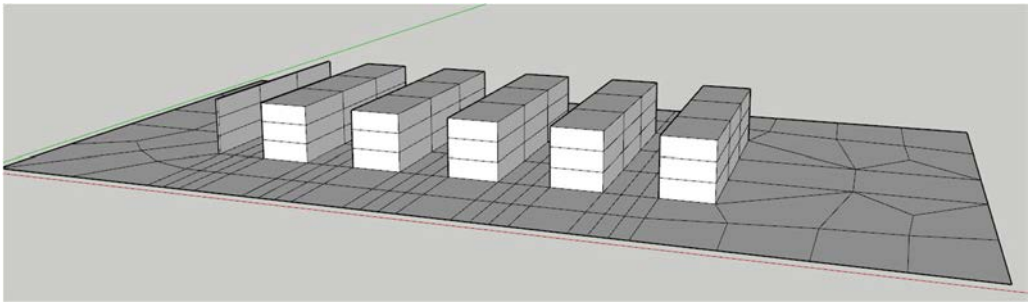

Figure 2. Digital mock-up of the climabat experiment.

The numerical model requires a set number of parameters describing the heat exchanges occurring during the simulation, and a certain range of inputs including meteorological data (boundary conditions). The goal is to determine the missing parameters from the measurements and to approximate the measurements both inside and outside the buildings.

Table 1. Thermal characteristics determined by previous studies

Materials	Concrete container	Slab mortar	Graveled concrete
Thermal conductivity (W/(m.K))	2.36	2.05	3.58
Thermal capacity (kJ/(kg.K))	918	695	926
Density (kg/m^3)	2150	2780	2290

Three indicators stand out for microclimate model validation (Pigliautile et al., 2020, p.) (Detommaso et al., 2021) and are given Table 2.

Table 2 Error metrics for model evaluation

Index	Name	Formula
RMSE	Root Mean Square Error	$\sqrt{\frac{\sum_{i=1}^{n}(m_i - s_i)^2}{n}}$
NMBE	Normalized Mean Bias Error	$\frac{1}{\overline{m}}\frac{\sum_{i=1}^{n}(s_i - m_i)}{n}$
d	Index of agreement	$1 - \frac{\sum_{i=1}^{n}(s_i - m_i)^2}{\sum_{i=1}^{n}(\lvert s_i - \overline{m}\rvert + \lvert m_i - \overline{m}\rvert)^2}$

The input for the air temperature is the measurements from the meteorological station placed on the nearby roof. The measurements indicate at hot period with three days reaching a temperature of 35°C and mainly above 25°C at the hottest time of the day. The canyon air

temperature measurements reach an average overheating of 4°C compared to the roof as highlighted by Djedjig et al. (2015). A pyrgeometer in the roofs measures the longwave incoming radiation from the sky, which is used as the equivalent sky temperature for each surface weighted by its view factor to the sky. A pyrgeometer above the canopy facing the ground allows the emissivity of surfaces to be calibrated. The sensor sees two materials, so two emissivities are considered. A 2D model canyon for the reference canyon (Figure 1) allows us to formulate the minimization problem Equation 1 where we estimate emitted infrared radiation from the surface temperatures, and compare them with the pyrgeometer measurements by calculating the mean squared error for the whole period.

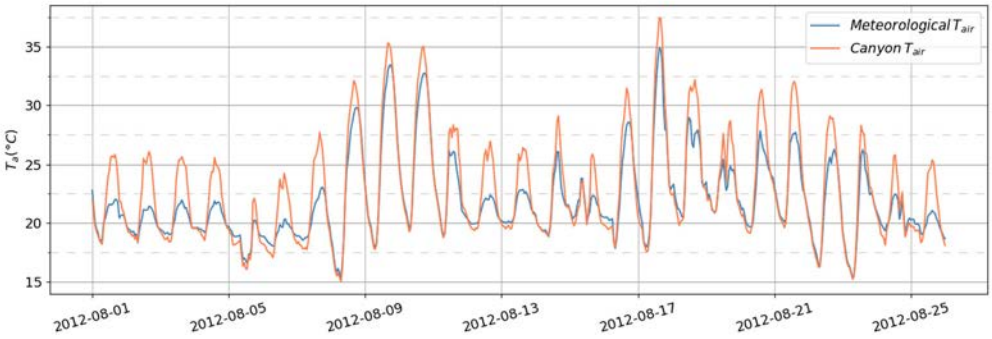

Figure 3. Meteorological and inside canyon measured air temperatures

The incoming solar radiation of SOLENE is calibrated with the pyranometer on the roof by applying a time dependent coefficient between the measured and the calculated solar radiation on a horizontal plane. The buildings are equipped with a white coating of known albedo. The pyranometer above the canyon allows verifying this information as well as determining the albedo of the ground. An imaginary surface is added to the digital mock-up to calculate the view factors towards it. The RMSE for the full period at 5-min time step is 13.57 W/m^2. We apply a similar methodology as for the emissivities to verify the albedo for both the ground and for the walls based on the measurements of the pyranometer. This step is necessary as white paint degradation can occur.

Equation 1. Emissivity optimization formulated problem, $R^2 = 0.99$

$$\min_{\varepsilon_{wall},\, \varepsilon_{ground}} \left(\sum_{timestep} \left(LW_{pyrgeo} - \sigma \sum_{surface\ i} \varepsilon_i VF_{i\to j} T_{s,i}^4 \right) \right)^2$$

For the wind speed calculation, a wind profile is specified in QUIC, which calculates wind speed in 36 directions for a reference wind speed.

Equation 2 gives the wind profile, a decay parameter a_{can} is determined from the geometry of climabat according to Cionco (1965). For the meteorological wind speed, the same relationship is applied by arbitrarily choosing a_{can} equal to one. This value should be determined by the morphology of the surrounding area. Another possibility is to use measurements from the in-situ anemometer and from the roof anemometer to determine a linear relationship between these two quantities. The transformed wind speed could then be used as the meteorological input to the methodology using the results of QUIC. To verify this methodology, the correlation between the calculated wind speed and the roof wind speed could be compared to the correlation obtained from measurements when data are available.

Equation 2. Input QUIC wind velocity profile

$$U = \begin{cases} U(H)e^{a_{\text{can}}\left(\frac{z}{H}-1\right)} \; if \; z \leq H \\ U_{ref}\dfrac{\ln\left(\frac{z-d}{z_0}\right)}{\ln\left(\frac{Z_{ref}}{z_0}\right)} \; if \; z > H \end{cases}$$

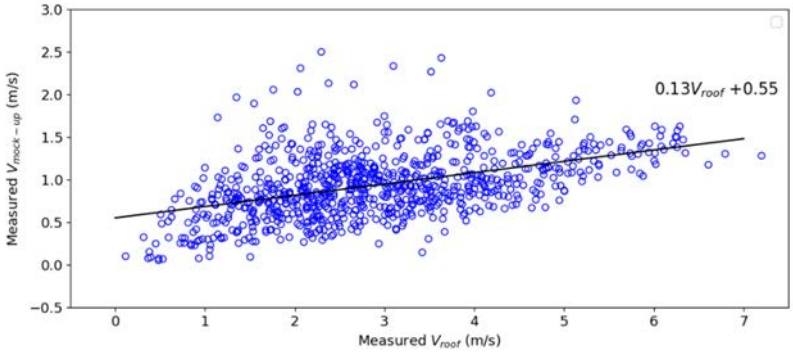

Figure 4. Measured relation between wind speed velocity at roof level and at the mockup

Conductivity, thermal capacity and density of the walls were determined in a previous study in the laboratory (see Table 1). However, the two parameters that remain are the heat transfer coefficient inside and outside of the buildings. To determine the internal convective heat transfer coefficient, we use a model of the DIMOSIM thermal zone where we impose internal surface temperatures from measurements. The latter recalculates the air temperature and the mean radiant temperature, and take *CHTC* as input. This part is calibrated manually but could be optimized in a future study. For the exterior *CHTC*, we consider the formula proposed by Palyvos (2008) : $h_{conv,ext} = 5.7 + 3.8*V_W$ where V_W is the wind speed at the monitored surface ,with a measured mean in-situ wind speed of 0.84 m/s as shown above (see Figure 4). We use the measured wind speed at the anemometer's position because the variation of the external convection coefficient as a function of the adjacent wind speed is not yet implemented in the model. The available measurements also allow the determination of the outdoor *CHTC*. Table 3 summarizes all of the parameters discussed above.

Several thermocouples are placed under the slab and used as boundary conditions for the subsurface temperature. The next step in the calibration procedure is to optimize the thermal properties of the soil to obtain a unique boundary condition for the subsurface temperature. In this study, we do not validate humidity calculation. This variable could help to validate the velocity field since without a moisture source; the calculation of the specific depends only on the outdoor airflow.

Table 3. Thermal properties of determined surface elements

ε_{ground}	ε_{walls}	$h_{conv,ext}$	ρ_{ground}	ρ_{walls}	$h_{conv,int,walls}$	$h_{conv,int,inner}$	$h_{conv,int,ground}$
0.96	1.0	8.9	0.35	0.64	8.0	2.0	1.0

The calibration process is ongoing but we would like to illustrate the capabilities of the model to evaluate mitigation scenarios for indoor and outdoor environments. We perform three simulations to evaluate the capacity of cooling materials in the canyon with the presence of air conditioning where the flow is directed into the canopy cells.

Mitigation scenarios

At this stage of validation, we evaluate the effect of reflective paintings on the potential mitigation of energy consumption related to air-conditioning as well as the rise of the air temperature in the canyon. The air conditioning of a thermal zone considers the air temperature of the adjacent air cells, and thus a more realistic consideration of the operating conditions. We evaluate three reflectivity scenarios: the albedo of the walls is either 0.3 (low), 0.63(high) or 0.85 (very high) with and without air conditioning to evaluate the effect on the canyon microclimate and building energy performance. The cooling set point for operative temperature is 26°C.

Results and Discussion

Calibration

The prediction capability of the model is evaluated by comparing outdoor air temperature of the canyon, indoor air temperature of the building, as well as the interior and exterior surface temperatures of a façade. We compute errors for every hour of the period August 1-26 that corresponds to 601 data points and is summarized in Table 4.

Table 4. Error metrics based on measurements and microclimate simulation

	RMSE	MBE	d
$T_{air,\ canyon}$ (°C)	1.28	0.18	0.977
$T_{air,\ indoor}$ (°C)	1.26	-0.98	0.98
Φ_{LW} (W/m^2)	11.9	-9.54	0.964
$T_{s,\ east\ wall}$ (°C)	1.28	0.35	0.979
$T_{s,\ west\ wall}$ (°C)	1.97	-0.005	0.871

The average error for outdoor air temperature by hour is shown in Figure 5. The mean error remains within a range of 1.5 degrees and the standard deviation seems to increase with temperature. On average, the model underestimates the air temperature by up to 1°C during the day and overestimates it by up to 1.7°C at night. However, there appears to be no bias as indicated by the MBE.

The indoor air temperature is close to the value calculated by the model of a thermal zone, which is informed by the measurements, which underestimates the air temperature, as indicated by a MBE of -0.98°C for the microclimate simulation, and an MBE of -0.38°C and a RMSE of 0.46°C for the thermal zone during calibration phase.

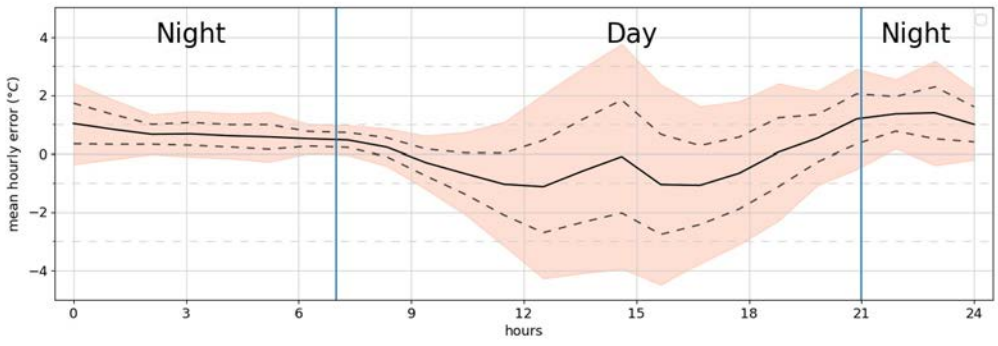

Figure 5. Exterior air temperature average hourly error mean and standard deviation

Mitigation scenarios

As shown in Table 5, the increase of albedo on either with or without air conditioning diminishes the energy consumption or cooling degree hours. However, the reflectivity of the roof also changes; the benefits are expected to be far less if the roof is not affected. The use of air conditioning affects microclimate. Daily maximum increase of air temperature for August 1-26 is depicted on Figure 6 as well as the average cooling demand with respect to average air temperature of the canyon. The relative difference on energy performance between low and very high albedo is because the building is not insulated with a U-value of 3.9 W/(m^2.K). Air conditioning could also affect the mean radiant temperature (MRT) by modifying the wall temperatures as shown in Figure 6. The AC cools the wall for low reflectivity by decreasing by 3°C the outdoor surface temperature and thus reducing the infrared portion of the MRT. For very high albedo, the AC has almost any effect in surface temperature. We can expect to see almost any effect with an insulated wall.

Table 5. Thermal Load and Cooling Degree Hours

Scenario	Low albedo	High albedo	Very high albedo
Total Thermal Load (MWh)	7.2	2.2	0.30
Cooling Degree Hours (CDH)	3068	765	111

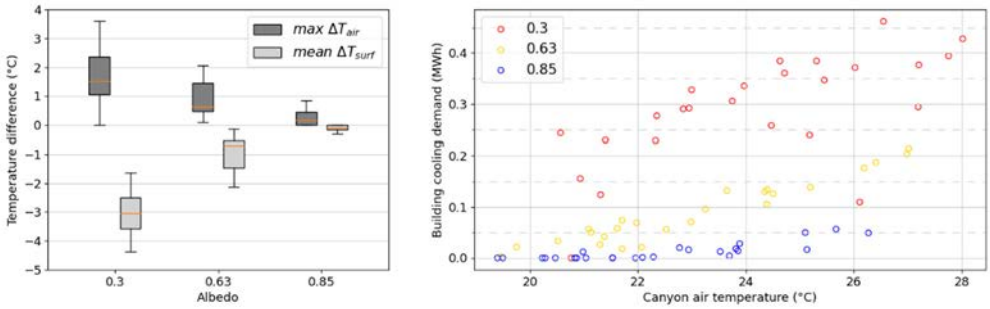

Figure 6. Boxplots of air and wall temperatures difference in the canyon with and without an AC (left) and energy signature of the building (right) for the three scenarios of reflectivity

Conclusion and perspectives

This work presents a methodology to evaluate a microclimate model coupled to an UBEM as well for both indoor and outdoor conditions. The methodology is based on measurements of microclimate variables made on a reduced scale mockup that does not have the uncertainties of a real neighborhood. To characterize the numerical model, several parameters are determined from the measurements. Finally, the capabilities of the model are evaluated with common error metrics and a brief analysis for air temperatures. Wind speed, which is a critical parameter, is difficult to evaluate due to the availability of measurements. However, the influence of the wind field, mainly the wind direction, will be studied to evaluate the ability of the model to correctly represent the canyon effect. Another aspect concerns the subsurface temperature, which needs to be calibrated and be unique to the entire mock-up and less dependent on the surface temperature of the slab. Finally, the outdoor convective heat transfer coefficient will be determined.

Three scenarios of cool paints with an indoor temperature set point of 26°C accompanied by an AC heat flux shows a exacerbation of the air temperature which diminishes as the reflectivity of the walls increases. A future study will consist in analyzing other cooling solutions, including green walls, as well as modifying the insulation and the inertia of the building. Additional criteria such as radiation and humidity will allow for a more detailed assessment of outdoor thermal comfort in relation to building performance.

Acknowledgments

This work was supported by the CSTB (Centre Scientifique et Technique du Bâtiment) Research Program.

Nomenclature

Symbol	*Quantity*	*[SI unit]*
a_{can}	Canopy attenuation coefficient	dimensionless
A	Surface area	[m^2]
h_{conv}	Convective heat transfer coefficient	[$W/(m^2K)$]
H	Buildings height	[m]
T_{air}	Air temperature	[°C]
$T_{s,i}$	Surface temperature of surface I	[°C]
$VF_{i\rightarrow j}$	View Factors from surface i to j	dimensionless
V_W	Wind speed at monitored surface	[m/s]
z	Height	[m]
z_{ref}	Reference height	[m]
z_0	Roughness length	[m]
ε	Emissivity	dimensionless
λ_f	Frontal area index	[m^2/m^2]
ρ_{albedo}	Ground albedo	dimensionless
Φ_{LW}	Infrared radiation flux	[W/m^2]

References

Allegrini, J., Dorer, V., & Carmeliet, J. (2012). Influence of the urban microclimate in street canyons on the energy demand for space cooling and heating of buildings. Energy and Buildings, 55, 823-832. https://doi.org/10.1016/j.enbuild.2012.10.013

Athamena, K., Sini, J.-F., Rosant, J.-M., & Guilhot, J. (2018). Numerical coupling model to compute the microclimate parameters inside a street canyon : Part II: Experimental validation of air temperature and airflow. Solar Energy, 170, 470-485. https://doi.org/10.1016/j.solener.2018.05.015

Cionco, R. M. (1965). A Mathematical Model for Air Flow in a Vegetative Canopy. Journal of Applied Meteorology, 4(4), 517-522. https://doi.org/10.1175/1520-0450(1965)004<0517:AMMFAF>2.0.CO;2

Detommaso, M., Costanzo, V., & Nocera, F. (2021). Application of weather data morphing for calibration of urban ENVI-met microclimate models. Results and critical issues. Urban Climate, 38, 100895. https://doi.org/10.1016/j.uclim.2021.100895

Djedjig, R., Bozonnet, E., & Belarbi, R. (2015). Experimental study of the urban microclimate mitigation potential of green roofs and green walls in street canyons. International Journal of Low-Carbon Technologies, 10(1), 34-44. https://doi.org/10.1093/ijlct/ctt019

Doya, M., Bozonnet, E., & Allard, F. (2012). Experimental measurement of cool facades' performance in a dense urban environment. Energy and Buildings, 55, 42-50. https://doi.org/10.1016/j.enbuild.2011.11.001

Erell, E., Pearlmutter, D., Boneh, D., & Kutiel, P. B. (2014). Effect of high-albedo materials on pedestrian heat stress in urban street canyons. Urban Climate, 10, 367-386. https://doi.org/10.1016/j.uclim.2013.10.005

Garreau, E., Abdelouadoud, Y., Herrera, E., Keilholz, W., Kyriakodis, G.-E., Partenay, V., & Riederer, P. (2021). District MOdeller and SIMulator (DIMOSIM) – A dynamic simulation platform based on a bottom-up approach for district and territory energetic assessment. Energy and Buildings, 251, 111354. https://doi.org/10.1016/j.enbuild.2021.111354

Groleau, D., Fragnaud, F., & Rosant, J.-M. (2003). Simulation of the Radiative Behavior of an Urban Quarter of Marseille with the Solene Model. Proceedings from ICUC-5: Fifth International Conference on Urban Climate. Lodz (Poland).

Krayenhoff, E. S., Broadbent, A. M., Zhao, L., Georgescu, M., Middel, A., Voogt, J. A., … Erell, E. (2021). Cooling hot cities : A systematic and critical review of the numerical modelling literature. Environmental Research Letters, 16(5), 053007. https://doi.org/10.1088/1748-9326/abdcf1

Kyriakodis, G.-E. (2020). Development of a coupled simulation tool for urban building energy demand, district energy systems and microclimate modeling. (Theses, Universite de La Rochelle). Universite de La Rochelle. Consulté à l'adresse https://hal.archives-ouvertes.fr/tel-03203724

Mao, J., Fu, Y., Afshari, A., Armstrong, P. R., & Norford, L. K. (2018). Optimization-aided calibration of an urban microclimate model under uncertainty. Building and Environment, 143, 390-403. https://doi.org/10.1016/j.buildenv.2018.07.034

Palyvos, J. A. (2008). A survey of wind convection coefficient correlations for building envelope energy systems' modeling. Applied Thermal Engineering, 28(8), 801-808. https://doi.org/10.1016/j.applthermaleng.2007.12.005

Pigliautile, I., Chàfer, M., Pisello, A. L., Pérez, G., & Cabeza, L. F. (2020). Inter-building assessment of urban heat island mitigation strategies : Field tests and numerical modelling in a simplified-geometry experimental set-up. Renewable Energy, 147, 1663-1675. https://doi.org/10.1016/j.renene.2019.09.082

Salvati, A., Kolokotroni, M., Kotopouleas, A., Watkins, R., Giridharan, R., & Nikolopoulou, M. (2022). Impact of reflective materials on urban canyon albedo, outdoor and indoor microclimates. Building and Environment, 207, 108459. https://doi.org/10.1016/j.buildenv.2021.108459

Singh, B., Hansen, B. S., Brown, M. J., & Pardyjak, E. R. (2008). Evaluation of the QUIC-URB fast response urban wind model for a cubical building array and wide building street canyon. Environmental Fluid Mechanics, 8(4), 281-312. https://doi.org/10.1007/s10652-008-9084-5